

# Statistical optimization of bile salt deployed nanovesicles as a potential platform for oral delivery of piperine: accentuated antiviral and anti-inflammatory activity in MERS-CoV challenged mice

Mohamed Y. Zakaria<sup>a</sup>, Eman Fayad<sup>b</sup>, Fayez Althobaiti<sup>b</sup>, Islam Zaki<sup>c</sup> and Ali H. Abu Almaaty<sup>d</sup>

<sup>a</sup>Department of Pharmaceutics and Industrial Pharmacy, Faculty of Pharmacy, Port Said University, Port Said, Egypt; <sup>b</sup>Department of Biotechnology, Faculty of Sciences, Taif University, Taif, Saudi Arabia; <sup>c</sup>Department of Pharmaceutical Organic Chemistry, Faculty of Pharmacy, Port Said University, Port Said, Egypt; <sup>d</sup>Department of Zoology, Faculty of Science, Port Said University, Port Said, Egypt

## ABSTRACT

The objective of this paper is to confine piperine, a poor oral bioavailable herbal drug into bile salt based nano vesicles for improving its aqueous solubility, hence, its therapeutic activity. Piperine-loaded bilosomes were fabricated adopting thin film hydration technique according to  $3^2.2^1$  full factorial design to investigate the impact of different formulation variables on the characters of bilosomes: entrapment efficiency (EE%), particle size, and % of drug released post 8 h (Q8hr). The selected optimum formula was F2 (enclosing 1% bile salt, brij72 as a surfactant, and ratio of surfactant:cholesterol was 9:1) with desirability value 0.801, exhibiting high EE% ( $97.2 \pm 0.8\%$ ) nanosized spherical vesicles ( $220.2 \pm 20.5$  nm) and Q8hr ( $88.2\% \pm 5.6$ ). The superiority of the optimized formula (F2) over the drug suspension was revealed via *ex vivo* permeation study, also pharmacokinetic study denoted to the boosted oral bioavailability of piperine-loaded bilosome compared to piperine suspension. Moreover, antiviral activity and safety margin of F2 was significantly higher than that of the drug suspension. The ability of piperine to interact with the key amino acids in the receptor binding domain 4LN as indicated by its docking configuration, rationalized its observed activity. Furthermore, F2 significantly reduce oxidant markers, inflammatory cytokines in MERS-CoV-infected mice. Hence, bilosomes can be considered as a carrier of choice for piperine with potential antiviral and anti-inflammatory activities.

## ARTICLE HISTORY

Received 12 April 2021  
Revised 16 May 2021  
Accepted 18 May 2021

## KEYWORDS



Piperine bilosomes; optimization; anti-MERS-CoV activity; molecular docking; inflammatory cytokines; pharmacokinetic study

## 1. Introduction

Middle East respiratory syndrome coronavirus (MERS-CoV) was initially concealed as a recent coronavirus leading to a tragic manifestation of acute respiratory distress syndrome and renal failure in 2012 (Iwata-Yoshikawa et al., 2019). The gravity of the consequences not only limited on respiratory distress syndrome (ARDS) but may cause multi organ failure, and death with a grade of severity hitting 35% (Li & McCray, 2020). Moreover, its high and rapid human-to-human respiratory transmission boost its potential to be pandemic (Cockrell et al., 2017). With the emergence of COVID-19 pandemic, another member of the family of Coronaviridae along with MERS-CoV and SARS-CoV-1 that give rise to severe respiratory syndrome compel the rise up of novel antivirals possessing high safety and efficacy (Mrityunjaya et al., 2020). Vast combinations which were employed in treatment of SARS CoV or Middle East respiratory syndrome (MERS) coronavirus or and human immunodeficiency virus (HIV) patients were also investigated in some exploratory studies as a potential remedy for COVID-19-infected patients (Lu, n.d.). Owing to the relative biosafety, availability of more chiral centers,

presence of structural and chemical diversity in the natural compounds, thus, they can be deemed as an outstanding source of drugs in enormous diseases especially the viral infections (Mishra et al., 2020).

Piperine is an alkaloid compound allied to Piperaceae family (black pepper) that is in charge of the pungent taste of many pepper species (Chopra et al., 2016). Piperine is conventionally used in treatment of various gastrointestinal upsets, as well as for neurological and broncho-pulmonary disorders (asthma and chronic bronchitis) (Stojanović-Radić et al., 2019). Piperine encompasses wide spectrum of physiological activities including antioxidant, antimicrobial (Alshehri et al., 2020), anti-asthmatic, antitumor, and especially vigorous anti-inflammatory role, hence, it can be reclaimed for suppression of MERS and COVID-19 induced hyper inflammation (Damanhour, 2014; Mrityunjaya et al., 2020). Unfortunately, its clinical applications are impeded by its hydrophobicity and low stability and rapid metabolism, hence, poor bioavailability (Ding et al., 2018; Imam et al., 2020). These pitfalls can be overwhelmed by the manipulation of the bioactive vesicular carriers. Liposomes and

**CONTACT** Mohamed Y. Zakaria  [dr\\_m\\_yehia@live.com](mailto:dr_m_yehia@live.com)  Department of Pharmaceutics and Industrial Pharmacy, Faculty of Pharmacy, Port Said University, Port Said 42526, Egypt

This article has been corrected with minor changes. These changes do not impact the academic content of the article.

© 2021 The Author(s). Published by Informa UK Limited, trading as Taylor & Francis Group.

This is an Open Access article distributed under the terms of the Creative Commons Attribution-NonCommercial License (<http://creativecommons.org/licenses/by-nc/4.0/>), which permits unrestricted non-commercial use, distribution, and reproduction in any medium, provided the original work is properly cited.

niosomes are conventionally used vesicles to sheath drugs. Woefully, their restricted encapsulation efficiency and limited stability, and scaling up problems, the requisite for evolving novel vesicular systems was aroused (Ammar et al., 2018a). Bile salts (BS) encompassing vesicles or bilosomes have been developed as a modification for liposomes and niosomes which offer more stable vesicles by addition of BS to the lipid bilayers (Aburahma, 2014). Many attempts have been evolved exposing the positive impact of tailoring oral bilosomes bearing sparsely water soluble drugs and vaccines by the virtue of its high stability in counteracting the harsh circumstances in GIT (Aburahma, 2014).

In the current study, piperine oral bioavailability was aspired to be promoted via fabrication of different bilosomal formulae charged with piperine adopting various variables in  $3^2.2^1$  full factorial design. The optimal bilosomal formula was evaluated for its morphology. Finally, pharmacokinetic and pharmacodynamics study were conducted to assess the efficacy and the boosted bioavailability of the optimal piperine-loaded bilosomal system, therefore, improving piperine antiviral and anti-inflammatory activity against MER-CoV infection and its subsequent lung inflammation.

## 2. Material and methods

### 2.1. Material

Piperine, span65, were purchased from Sigma-Aldrich Chemical Co. (St. Louis, MO). Brij72, Brij78, and sodium deoxycholate was purchased from BASF Co. (Florham Park, NJ). Cholesterol was obtained from ITX Biomedicals (Santa Ana, CA). Sodium hydroxide, potassium dihydrogen orthophosphate, and absolute ethanol were purchased from El-Nasr Chemical Co., Cairo, Egypt. Spectra/Pore® dialysis membrane (12,000–14,000 molecular weight cut off) was purchased from Spectrum Laboratories Inc., Los Angeles, CA. All chemicals and solvents were of analytical grade and were used as received. Serum biomarkers kits were purchased from Sigma-Aldrich Chemical Co. (St. Louis, MO). Specific ELISA kits were purchased from eBioscience Co. (San Diego, CA).

### 2.2. Fabrication of piperine-loaded bilosomes

Spare modifications were adhered to thin film hydration technique which was adopted for the development of piperine-loaded bilosomes (Al-mahallawi et al., 2015). Briefly, piperine (20 mg), the surfactant (Span 65, Brij 72, or Brij 78) and cholesterol in different ratios (9:1 or 5:5) were dissolved in 10 ml ethanol in a round bottom flask (Table 1) using an ultrasonic bath sonicator (Ultra Sonicator, Model LC 60/H Elma, Singen, Germany) for 10 min. Then the attained organic solution was dispelled at 60 °C under reduced pressure for

**Table 1.**  $3^2.2^1$  full factorial design manipulated for optimization of the piperine-loaded bilosomal formulae.

Factors (independent variables)	Levels		
X1: Type of surfactant	Span 65	Brij 72	Brij78
X2: Surfactant:cholesterol ratio	9:1		1:1
X3: Concentration of bile salt (%)	1	2.5	5

30 min utilizing a rotary evaporator (Rotavapor, Heidolph VV 2000; Heidolph Instruments, Kehlheim, Germany) up till the formation of completely dry thin film. Formerly the attained dry film was hydrated using 10 ml phosphate buffer solution encompassing the bile salt (SDC), for 2 h to cast a crude piperine-loaded bilosomal dispersion. Furthermore, the bilosomal dispersions were subjected to sonication for 10 min in a bath sonicator at room temperature aspiring for further subside in particle size. The attained formulae were kept at 4 °C for further characterization.

### 2.3. In vitro characterization and optimization of piperine-loaded bilosomes

#### 2.3.1. Entrapment efficiency percent (EE%)

To appraise the percentage of piperine embedded within the formulated bilosomal dispersion, precisely; 1 ml of piperine-loaded bilosomal dispersion (resembling 2 mg of the drug) diluted with 5 mL distilled water and manually agitated for 2 min. Cooling centrifugation technique for 1 h was used to decouple the unenclosed piperine from piperine-loaded bilosome at 15,000 rpm and 4 °C (Beckman, Fullerton, Canada) (Ammar et al., 2018b). The sedimented vesicles were harvested away, rinsed twice with distilled water, and centrifuged again for 30 min. The sonication of the separated particles using methanol was performed to predict the amount of the encompassed piperine. The concentration of the enclosed piperine within the vesicles was allocated spectrophotometrically at  $\lambda_{max}$  340 nm versus ethanol as blank. EE% was calculated as follows:

$$\% \text{ of piperine entrapped} =$$

$$\left( \frac{\text{Amount of piperine entrapped}}{\text{Total amount of piperine}} \right) \times 100 \quad (1)$$

#### 2.3.2. Exploration of vesicle size, PDI, and zeta potential (ZP)

The fabricated piperine-loaded bilosomes droplet size, ZP, and PDI were investigated utilizing Mastersizer (Malvern Instruments, Malvern, UK). About 0.1 ml of piperine-loaded bilosomal dispersion was diluted with 10 ml distilled water in a glass tube and shaken manually for 5 min. Dynamic laser scattering technique was manipulated to determine the distribution size at 25 °C using 45 mm focus lens and a beam length of 2.4 mm. The test was performed in triplicates (Albash et al., 2019).

#### 2.3.3. In vitro piperine release

Around 1 ml of each of the formulated piperine-loaded bilosomal formulae was diluted to 2 ml sorenson phosphate buffer (pH 7.4), then (1 mL) equivalent to 1 mg piperine from the diluted particle dispersion was conveyed to a 10 cm in length and 2.5 cm in diameter glass cylinder and a presoaked cellulose membrane was allocated at its bottom where the dispersion was prevailed over. The glass cylinder was

mounted on the shaft of the dissolution tester (Copley, DIS 8000, Nottingham, UK) and hanged in 900 ml dissolution media (sorensen phosphate buffer, pH 7.4) at  $37 \pm 0.5^\circ\text{C}$  and speed of 50 rpm (Mohammed et al., 2020). At scheduled time interventions, equal volumes were withdrawn and the percent drug released was detected spectrophotometrically at 342 nm. *In vitro* piperine release was carried out in triplicates.

Depending on the maximum EE%, Q8hr and minimum globule size, the optimum piperine bilosome formula was picked. Statistical analysis of the data was implemented using Design Expert® 7 software (Stateese, Minneapolis, MN) and the best formula with the elevated desirability value was picked for furthermore evaluations.

## 2.4. *In vitro* characterization of the optimum lyophilized piperine-loaded bilosomal formula

The optimum piperine-loaded bilosomal formula was solidified adopting lyophilization technique (Alpha 2-4, CHRIST, Osterodeam Harz, Germany), where lysis of the vesicles was hindered using mannitol (5% w/v) as lyoprotectant. Furthermore, bilosomal suspension was freezed over night at  $-80^\circ\text{C}$  and dried for a period of 24 h under vacuum (Elnaggar et al., 2019). The freeze-dried bilosomal powder was kept in a firmly closed glass tube in a desiccator for furthermore analysis.

### 2.4.1. Differential scanning calorimetry (DSC)

DSC-50 (Shimadzu, Kyoto, Japan) was manipulated to evaluate the thermal attitude of pure piperine, plain optimum formula, piperine-loaded bilosome, and cholesterol. The calibration of the equipment was performed using purified indium (99.9%). About that  $10^\circ\text{C}$  was elevated each minute, surrounded by nitrogen in a temperature range of 20– $400^\circ\text{C}$  (Mohammed et al., 2020).

### 2.4.2. Transmission electron microscopy (TEM)

The configuration of the optimal bilosomal formula was investigated by TEM (Joel JEM 1230, Tokyo, Japan). The stained vesicles' dispersion was attached on a carbon grid with copper coat and kept to dry to get a thin film. The sheet of copper was entered into the TEM (Abdellatif et al., 2017).

### 2.4.3. Effect of storage on the *in vitro* characters of the optimized formula

The optimal formula was reserved at  $4^\circ\text{C}$  and  $25^\circ\text{C}$  for 3 and 6 months. Samples from each formulation were taken at 0, 3, and 6 months. The stability was assessed with respect to EE%, particle size, and Q8hr, and the results of those parameters were subjected to ANOVA statistical analysis and  $p < .05$  was selected as a level of significance (Albash et al., 2019).

## 2.5. *Ex vivo* drug gut permeation study

Non-everted gut sac technique was adopted in the assessment of *ex vivo* intestinal transport study of the optimum formula compared with the drug suspension as reported in previous studies (Saifi et al., 2020). Twelve male Wistar rats (weighing 170–250 g) were subjected to anesthesia utilizing diethyl ether after being kept under overnight fasting and then they were sacrificed through cervical dislocation. The small intestine was extracted surgically, and a slice of 5 cm long section was obtained and rinsed with normal saline to wash out any food residues. The intestinal segments were rinsed with 2 ml of Krebs–Ringer solution. The cleaned gut after closing the lower end of the sac by a thread by using a blunt ended syringe, each sac was filled with an estimated volume from piperine suspension (compressing 5 mg piperine) or what equivalent to 5 mg of piperine entrapped in the optimal bilosomal formula, finally the upper end was firmly closed by a thread. Each sac was located in 50 ml of Krebs–Ringer solution in an organ bath. The system was continually aerated with 5%  $\text{CO}_2$  and 95%  $\text{O}_2$  and maintained at  $37 \pm 0.5^\circ\text{C}$  and stirred at 100 rpm. At a scheduled time, intervals (15, 30, 45, 60, 75, and 90 min) to compute the amount of piperine permeated, an aliquot of 2 ml of serosal medium was withdrawn. Then the samples were filtered through a 0.45- $\mu\text{m}$  pore size syringe filter, and piperine concentration permeated through the intestine was assessed by a HPLC (Hitachi LaChrome Elite, Tokyo, Japan) instrument that was equipped with a model series L-2000 organizer box, L-2300 column oven, L-2130 pump with built in degasser, Rheodyne 7725i injector with a 20 ml loop, and a L-2455 photo diode array detector (DAD), the wavelength was adjusted at 343 nm wavelength. Mobile phase composed of methanol-water (75:25) was pumped through C18 column at flow rate of 1 ml/min (Pachauri et al., 2015).

The apparent permeability (Papp) of piperine suspension and bilosomes were computed using the following formula:

$$p_{\text{app}} = (\text{cmmin}^{-1})F/A * c_0 \quad (2)$$

where  $F$  is the permeation flux,  $C_0$  is the initial concentration, and  $A$  is the total surface area of the ileum.

## 2.6. *In vitro* anti-MERS-CoV activity assessment

### 2.6.1. MTT cytotoxicity assay (TC50)

Dulbecco's Modified Eagle's Medium (DMEM) was utilized for sample dilution. About 10% DMSO in ddH<sub>2</sub>O was used to manipulate the stock solutions of the test compounds. The 3-(4,5-dimethylthiazol-2-yl)-2,5-diphenyltetrazolium bromide (MTT) method (Zhang et al., 2020) was adopted with slight modifications to assess the cytotoxic activity of the extracts that was investigated in Vero E6 cells. Concisely, the cells were harvested in 96 well-plates (100  $\mu\text{l}$ /well at a density of  $3 \times 10^5$  cells/ml) and the manipulated incubation circumstances was  $37^\circ\text{C}$  in 5% $\text{CO}_2$  for 24 h. Post 24 h, cells were served with vast concentrations of the tested compounds in triplicates. Another extra 24 h, the supernatant was disposed and cell monolayers were scrapped up with sterile phosphate

buffer saline (PBS) three times and each well was supplemented by MTT solution (20  $\mu$ l of 5 mg/ml stock solution) and incubated at 37 °C for 4 h succeeded by medium aspiration. About 200  $\mu$ l of acidified isopropanol (0.04 M HCl in absolute isopropanol = 0.073 ml HCL in 50 ml isopropanol) was utilized in each well to dissolved the yielded formazan crystals. The absorbance of formazan solutions were estimated at  $\lambda_{\max}$  540 nm with 620 nm as a reference wavelength using a multi-well plate reader. The percentage of cytotoxicity compared to the untreated cells was determined with the following equation. The plot of % cytotoxicity versus sample concentration was used to calculate the concentration which exhibited 50% cytotoxicity (TC50) (Henen et al., 2012):

$$\% \text{cytotoxicity} =$$

$$\frac{\left( \frac{\text{absorbance of cells without treatment} - \text{absorbance of cells with treatment}}{\text{absorbance of cells without treatment}} \right) \times 100}{\text{absorbance of cells without treatment}} \quad (3)$$

### 2.6.2. Plaque assay

MER-CoV titer was estimated via plaque assay loaded on Vero E6 cells. In accordance to previous studies, the assay was conducted using six well plate where Vero E6 cells ( $10^5$  cells/ml) were harvested at 37 °C for 24 h (Abou-Karam and Shier, 1990).  $10^3$  PFU/well was the yield of the dilution of Middle East respiratory syndrome-related coronavirus isolate NRCE-HKU270 (Accession no. KJ477103.2) virus and combined with the tested compounds utilizing its safe concentration and incubated for at 37 °C for 1 h, former of being aliened to the cells. Growth medium was decanted from the cell culture plates and the cells were inoculated with 100  $\mu$ l/well virus with the tested compounds, 1 h contact time for virus adsorption was conducted, the investigated compounds and 3 ml of DMEM after being supplemented with 2% agarose was aliened onto the cell monolayer; for the solidification, the plates were ported aside and incubated at 37 °C till evolution of viral plaques (3–4 days). Formalin (10%) was supplemented for 2 h followed by staining adopting 0.1% crystal violet in distilled water. Control wells were enclosed where untreated virus was incubated with Vero E6 cells and lastly plaques were casted and percentage reduction in plaques formation versus control wells was listed as the following:

$$\% \text{inhibition} = \frac{\text{viral count (untreated)} - \text{viral count (treated)}}{\text{viral count (untreated)}} \times 100 \quad (4)$$

## 2.7. Molecular docking study

A molecular docking study was conducted utilizing the MOE software program (MOE2009.10). The X-ray crystallographic structures of MERS-CoV receptor binding domain (RBD) (Chen et al., 2013) (PDB access code 4L3N) were acquired from the protein data bank (RCSB PDB, <https://www.rcsb.org>).

## 2.8. In vivo characterization of the picked piperine-loaded bilosome

### 2.8.1. Experimental animals and MERS-CoV viral infection

Forty female 10 weeks old female C57BL/6 mice ( $150 \pm 10$  g) were obtained from Biological Production Unit (BPU) of Theodore Bilharz Research Institute (Giza, Egypt) were accommodated for 7 days in standard polypropylene cages under standard laboratory conditions of temperature, humidity, and light 12 h of dark/light cycles with a free access to standard laboratory diet and water ad libitum as to reduce variation (Mohammed et al., 2020). The experimental protocol was approved by Research Ethics Committee, Port Said University. The animals were inoculated intranasally with 50  $\mu$ l of viral solution containing  $10^5$  p.f.u. resembling 50% tissue culture infectious dose (TCID<sub>50</sub>) of MERS-CoV (Iwata-Yoshikawa et al., 2019), then they were subdivided into four groups (10 mice in each group), and allocated randomly receiving different dosage regimen according to Table 2 their body weight and survival were monitored.

### 2.8.2. Estimation of the viral titer in acutely infected lungs via plaque assay

At days 3 and 6 post-infection, the animals were anesthetized by (1.6 g/kg) urethane and then sacrificed by overdose of Na pentobarbital (30–50 mg/kg IP). Furthermore, the lungs were harvested immediately after lightly rinsed with normal saline and dried with tissue paper. They were weighed accurately and homogenized using a glass tissue homogenizer (MPW-120 homogenizer, Bitlab, Shanghai, China) after the addition of 1 ml physiologic saline and with protease inhibitor (20 mM Tris-HCl, 150 mM NaCl, 1% Triton X-100, 0.1% SDS, Roche complete ULTRA Tablet) then centrifuged at 10,000 rpm for 10 min, the supernatant were frozen at –20 °C or –80 °C until analysis (Coates et al., 2018). Vero E6 cells were infected by serially diluted lung homogenate utilizing DMEM for 2 h at 37 °C. Twelve-well plates from the yielded Vero monolayers were challenged with 200  $\mu$ l/well serially diluted homogenate containing infectious virus and the assay was completed as previously discussed.

**Table 2.** Dosage regimen of different Wister rat groups used *in vivo* assessment.

Group number	Dosage regimen
Gp 1: Placebo (control)	Saline (2 ml/kg) intraperitoneally (i.p.) once then administered orally saline at dose of 5 ml/kg daily
Gp 2: MERS infected (untreated)	Intranasally infected with $10^5$ pfu/50 $\mu$ l of virus
Gp 3: Piperine suspension-treated GP	After infection an oral dose of 50 mg/kg (Selvendiran et al., 2006) once a day for 6 days
Gp 4: Piperine bilosome-treated GP	After infection an oral dose of 50 mg/kg (Selvendiran et al., 2006) once a day for 6 days



### 2.8.3. Estimation of cytokines and oxidative biomarkers induced by MERS-CoV infection

The animals were anesthetized by (1.6 g/kg) urethane and the blood and bronchial alveolar lavage fluid (BALF) were collected and prepared for further estimation of oxidative biomarkers and cytokines (Saadat et al., 2019). To prepare blood serum, 5 ml blood was collected from the animal heart after opening the chest in the test tube and centrifuged at 3500 rpm for 10 min (Saadat et al., 2019). The serum samples were collected and stored at  $-70^{\circ}\text{C}$  for measurement of the levels, malondialdehyde (MDA), and total thiol content (GSH). Meanwhile, to prepare BALF samples, according to a previous conducted study (Saadat et al., 2019), a cannula was located into the trachea and the right lung was washed with 1 ml normal saline for five times (totally, 5 ml) through a tracheal cannula. BALF was centrifuged at 2500 rpm at  $4^{\circ}\text{C}$  for 10 min. The supernatant was collected and stored at  $-70^{\circ}\text{C}$  for assessment of cytokines levels.

**2.8.3.1. Assessment of serum oxidant and antioxidant biomarkers.** Lipid peroxidation biomarker (MDA) level in serum was determined via thiobarbituric acid-reactive substances. The resulting pink colored chromogen was extracted with butanol and was measured at 532 nm (Shakeri et al., 2017). Estimation of glutathione (GSH) relies on the fact that both protein and non-protein thiol (SH-) groups (mainly GSH) react with Ellman's reagent [5,5'-dithiobis (2-nitrobenzoic acid)] to form a stable yellow color of 5-mercapto-2-nitrobenzoic acid, which can be measured colorimetrically at 412 nm (Shakeri et al., 2017).

**2.8.3.2. Assessment of IL-4 and IFN- $\gamma$  in BALF.** To estimate interleukin-4 (IL-4), interferon-gamma (IFN- $\gamma$ ), and precise ELISA kits (ebioscience Co, San Diego, CA) was adopted and the instructions provided by the manufacturer were utilized. Statistical analysis was carried out by ANOVA followed by Tukey's multiple comparisons test.

## 2.9. Pharmacokinetic study

The research protocol was in accordance and approved by Research Ethics Committee, Portsaid University. This study was conducted on male Wistar albino rats ( $n=12$ , weight range 220–250 g). Rats were housed in standard polypropylene cages six per cage under standard laboratory conditions of temperature, humidity, and light with a free access to standard laboratory diet and water ad libitum. The rats were divided into two groups of six rats each. Group I received the optimum piperine-loaded bilosome (F2), while group II received piperine suspension.

After overnight fasting, the rats were administered orally the optimum piperine-loaded bilosome and drug suspension with a dose equivalent to 20 mg/kg p.o. of piperine (Bajad et al., 2002). Post the oral administration, approximately 0.5 ml of blood was withdrawn from the tail vein at zero time and at (0.5, 1, 2, 4, 6, 8, 12, 18, and 24 h). Rats fed again 8 h after drug administration. The blood samples were gathered in EDTA coated tubes, then the plasma was separated directly

via centrifugation at 3500 rpm for 10 min and kept under  $-40^{\circ}\text{C}$  for further investigation. Piperine concentration was estimated by previously stated HPLC technique with slight modification.

The pharmacokinetic parameters of piperine from the investigate (piperine-loaded bilosome F2 and piperine suspension) were assessed for each rat by non-compartmental pharmacokinetic models using WinNonlin® pharmacokinetic software version 2.0 (Pharsight, Mountain View, CA).  $C_{\text{max}}$  and AUC<sub>0–24</sub> for both piperine-loaded bilosome F2 and piperine suspension were compared using the one-way ANOVA statistical test. In addition, the nonparametric signed-rank test (Mann–Whitney's test) was employed to compare the medians of  $T_{\text{max}}$  for the two treatment groups using the statistical software of Statistical Package for Social Sciences (SPSS) version 14 (SPSS, Chicago, IL). The difference at  $p < .05$  was considered significant (Albash et al., 2019).

## 3. Results and discussion

Bilosomes as a nano-vesicular carrier offers vast privileges over conventional vesicular carriers; superior stability, simplicity of manipulation, and high shelter efficiency facing the drastic circumstances in GIT (Aburahma, 2014). In the current study, different bilosomal formulae enclosing piperine were prosperously manipulated adopting thin film hydration technique utilizing various types of surfactants differ in their HLB (Span65, Brij 72, and Brij 78), bearing different surfactant:cholesterol ratio and different bile salt concentrations.

### 3.1. Experimental design statistical evaluation

$3^{2.2^1}$  full factorial designs were conducted to concurrently investigate the impact of formulation variables on the response as suggested. Here, 18 experimental runs were prevailed and their corresponding responses: EE%, particle size, and Q8hr in Table 3. The dependent variables were investigated according to two-factor interaction (2FI) model as it exploited the most prominent prediction  $R^2$  value. The adequate precision value of the model is used to confirm its adequacy to navigate the design space (Albash et al. 2019). A ratio higher than four is preferred which was noticed for all the dependent variables as illustrated in Table 4. The adjusted and predicted  $R^2$  should be within approximately 0.20 of each other to represent a reasonable agreement. As shown in Table 4, the predicted  $R^2$  values were in good harmony with the adjusted  $R^2$  in all the dependent variables except Q8hr. However, the response was not affected by any factor and this discrepancy was not thought to cause a bad impact on the whole model (Mosallam et al., 2021).

### 3.2. The influence of the variables on EE%

Eventually the estimation of entrapment efficiency offers a clue on the potential of the analyzed vesicles to enclose a significant amount of piperine. The percentage of piperine enclosed in the vesicles ranged from  $62.2 \pm 0.3\%$  to  $97.2 \pm 0.8\%$ . The impact of the variables, surfactant type (A),

**Table 3.** 3<sup>2</sup>.2<sup>1</sup> full factorial experimental design; experimental runs, independent variables, and measured responses of piperine-loaded bilosomes.

Formulae	X1	X2	X3	Y1 (%)	Y2 (nm)	Y3 (%)	Zp (MV)	PDI
F1	Span 65	9:1	1.00	93 ± 1.2	230.5 ± 15.2	79.4 ± 3.4	-39.1 ± 2.5	0.31 ± 0.08
F2	Brij 72	9:1	1.00	97.2 ± 0.8	220.2 ± 20.5	88.2 ± 5.6	-53.3 ± 5.4	0.22 ± 0.02
F3	Brij 78	9:1	1.00	90 ± 1.3	207.5 ± 18.3	90.1 ± 6.8	-49.1 ± 4.3	0.3 ± 0.05
F4	Span 65	5:5	1.00	87 ± 1.1	269.5 ± 24.4	94.3 ± 5.4	-43.1 ± 4.7	0.35 ± 0.07
F5	Brij 72	5:5	1.00	89.5 ± 0.7	250.9 ± 12.2	93.1 ± 3.5	-48.5 ± 5.4	0.4 ± 0.06
F6	Brij 78	5:5	1.00	84.2 ± 0.4	293.4 ± 21.1	102.3 ± 2.5	-51.1 ± 7.1	0.7 ± 0.14
F7	Span 65	9:1	2.50	88 ± 0.5	321.9 ± 23.5	83.2 ± 1.4	-42.2 ± 3.7	0.49 ± 0.05
F8	Brij 72	9:1	2.50	92.4 ± 1.9	311.4 ± 20.1	84.3 ± 1.9	-46.3 ± 3.6	0.5 ± 0.17
F9	Brij 78	9:1	2.50	84.3 ± 0.8	286.9 ± 13.7	88.2 ± 2.4	-48.9 ± 6.3	0.55 ± 0.08
F10	Span 65	5:5	2.50	82.5 ± 0.6	372.2 ± 15.6	90.5 ± 3.7	-32.3 ± 3.4	0.37 ± 0.07
F11	Brij 72	5:5	2.50	86.8 ± 0.9	354.5 ± 26.7	89.2 ± 5.6	-37.4 ± 4.5	0.64 ± 0.12
F12	Brij78	5:5	2.50	80.1 ± 0.7	343.1 ± 31.1	100.1 ± 4.5	-42.2 ± 4.5	0.53 ± 0.04
F13	Span 65	9:1	5.00	75.6 ± 1.8	189.2 ± 10.8	75.2 ± 4.8	-35.3 ± 3.7	0.49 ± 0.14
F14	Brij 72	9:1	5.00	79.3 ± 1.6	171.3 ± 15.2	92.1 ± 3.2	-40.2 ± 5.3	0.45 ± 0.07
F15	Brij78	9:1	5.00	72.1 ± 0.7	152.4 ± 20.5	81.4 ± 6.5	-44.4 ± 5.8	0.32 ± 0.03
F16	Span 65	5:5	5.00	65.2 ± 0.4	185.2 ± 19.8	96.3 ± 4.9	-47.2 ± 5.1	0.38 ± 0.05
F17	Brij 72	5:5	5.00	69.1 ± 0.6	143 ± 12.3	94.1 ± 1.2	-50.9 ± 6.2	0.57 ± 0.11
F18	Brij78	5:5	5.00	62.2 ± 0.3	131 ± 15.3	97 ± 2.9	-52.1 ± 5.9	0.42 ± 0.13

All values exploited as mean ± SD ( $n = 3$ ), Y1: entrapment efficiency percentage (EE%); Y2: particle size; Y3: % of piperine released after 8 h (Q8hr).

**Table 4.** 3<sup>2</sup>.2<sup>1</sup> Output factorial analysis data of piperine-loaded bilosomal formulae and the predicted and observed responses of the optimum formula (F2).

Responses	EE (%)	Particle size (nm)	Q8hr (%)
$R^2$	0.9996	0.9938	0.9581
Adjusted $R^2$	0.9983	0.9737	0.8219
Predicted $R^2$	0.9917	0.8745	0.1513
Adequate precision	94.986	21.355	9.52
Significant factors	X1, X2, X3	X1, X2, X3	X1, X2
Observed value of the optimal formula (F2)	97.2	220.2	88.2
Predicted value of the optimal formula (F2)	96.89	216	88.6

EE%: entrapment efficiency percentage; Q8hr: % of piperine released after 8 h.

surfactant:cholesterol ratio (B), and bile salt concentration (C) on EE% is displayed as 3D response plot in Figure 1(A). The ANOVA statistical analysis revealed that the impact of interaction AB and AC was non-significant ( $p > 0.05\%$ ), while that of BC was significant at ( $p = 0.001$ ) as the EE% of the formulae prepared using surfactant:cholesterol ratio 9:1 and bile salt concentration 1% with each surfactant type. The linear impact of each variable on the EE% was discussed as the following.

### 3.2.1. Influence of surfactant type on EE%

From Figure 2(A) and ANOVA results, it can be depicted that the EE% of the formulae prepared using Brij 72 (HLB 4.9,  $T_c = 44^\circ\text{C}$ ) was significantly higher ( $p < .0001$ ) than that of span 65 (HLB 2.1) and Brij 78 (HLB 15.3,  $T_c = 38^\circ\text{C}$ ) and this might be related to the HLB as proclaimed previously, the lower HLB value of nonionic surfactant predispose to a higher drug EE% (AbouSamra & Salama, 2017). Furthermore, the lipid phase transition temperature ( $T_c$ ) crucial role in investigating the influence of SAA on EE%. It was reported that the increase in the  $T_c$  will enhance the potential to fabricate highly compact vesicles leading to a higher EE% (Bnyan et al., 2018).

### 3.2.2. Influence of surfactant:cholesterol ratio

Never-less, the presence of cholesterol in the formulae lead to a positive impact on the vesicular structure and membrane fluidity as it fills in the voids in the vesicles, thus, promoting the EE%. From ANOVA statistical analysis, it was noticed that changing the surfactant: cholesterol ratio from

9:1 to 5:5 lead to a significant ( $p < .0001$ ) decline in the EE%. It may attributed to challenge aroused between cholesterol and piperine to be enclosed in the hydrophobic portions in the vesicles (Aboelwafa et al., 2010).

### 3.2.3. Influence of bile salt concentration

It was declared that increasing bile salt concentration will enhance the EE% (Saifi et al., 2020). From ANOVA statistical analysis data, it can be concluded that the EE% of formulae prepared with 1% SDC was significantly higher ( $p < .0001$ ) than that of formulae with 2.5% and 5%. This can be explained by the boost in the solubility of piperine in the formulated vesicular medium via the development of mixed micelles, high concentration of the bile salt increases the probability to act as solubilizing surfactant and decreases the compactness of the vesicles, hence, promoting the drug leakage rate and negatively impact the EE% (Ammar et al., 2018b).

### 3.3. Influence of variables on particle size

Particle size figures out to the fate of the drug in blood circulation as minute particles cannot be easily detected by the complements in the blood, moreover, it boosts the drug permeation, thus, enhancing the drug retention time and therapeutic activity. As illustrated in Table 3, the average particle size of the fabricated formulae ranged from  $131 \pm 15.3$  to  $372.2 \pm 15.6$  nm. The impact of the variables, surfactant type (A), surfactant:cholesterol ratio (B), and bile salt concentration

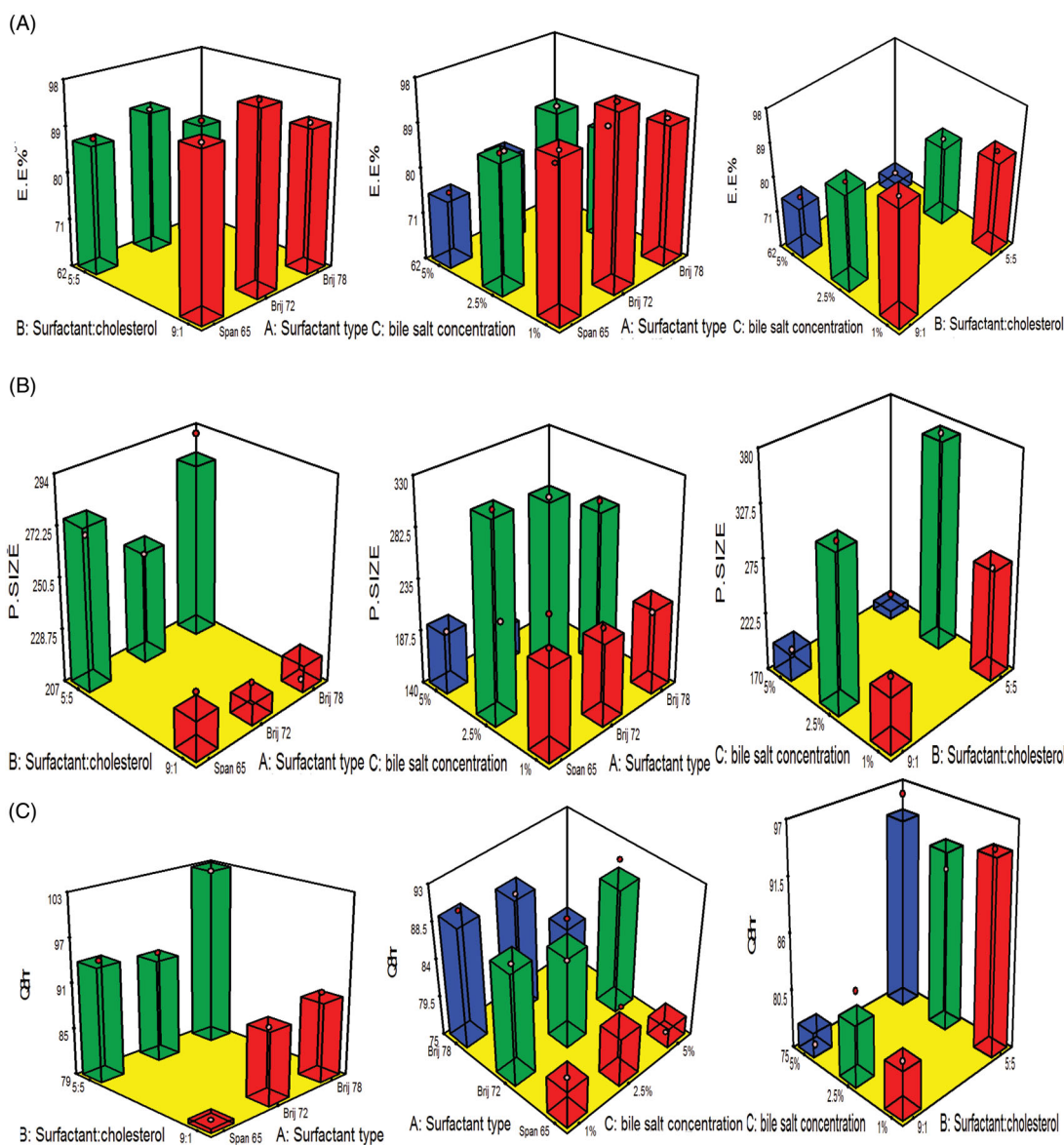


**Figure 1.** (A–C) 3D surface response plots showing interaction effects of independent variables on (A) EE%, (B) PS, and (C) Q8hr.

(C) on particle size is displayed as 3D response plot in Figure 1(B). The ANOVA statistical analysis revealed that the impact of interaction AB and AC was non-significant ( $p > .05$ ), while that of BC was significant at  $p = .0132$  as the particle size of the formulae prepared using surfactant:cholesterol ratio 9:1 was smaller than that of 5:5 at 1% and 2.5%, unfortunately, the reverse was happened at 5% bile salt concentration, this may be attributed to the combined effect of high level of both bile salt concentration and cholesterol predispose to increasing drug leakage, moreover, higher possibility of micelles formation and repulsion between vesicles due to accumulation of charges on the surface of the particles, hence, the suppression of particle size. The linear influence of each variable on particle size can be elucidated from the graphical representation in Figure 3 and was discussed as the following:

### 3.3.1. Influence of surfactant type

As claimed by many studies, as the drug entrapment increases, a corresponding increase in the particle size will be noticed, this can be accredited to the increment in the gap between the bilayers owing to the drug inclusion in the lipophilic voids in the vesicles (Hathout et al., 2007). This came in accordance to our results and confirmed by the results of ANOVA statistical analysis, where the particle size of the formulae prepared with Brij 72 and span 65 was significantly ( $p < .05$ ) greater than that of Brij 78.

### 3.3.2. Influence of surfactant:cholesterol ratio

The change in surfactant:cholesterol ratio from 9:1 to 5:5 predisposes to a significant ( $p = .0087$ ) increase in the average PS. The elevation in the amount of cholesterol impedes the tight compactness of the vesicles increasing the intermingling of the aqueous phase, thus, enlarge the particle size (Ramana et al., 2010). Moreover, the correlation between the

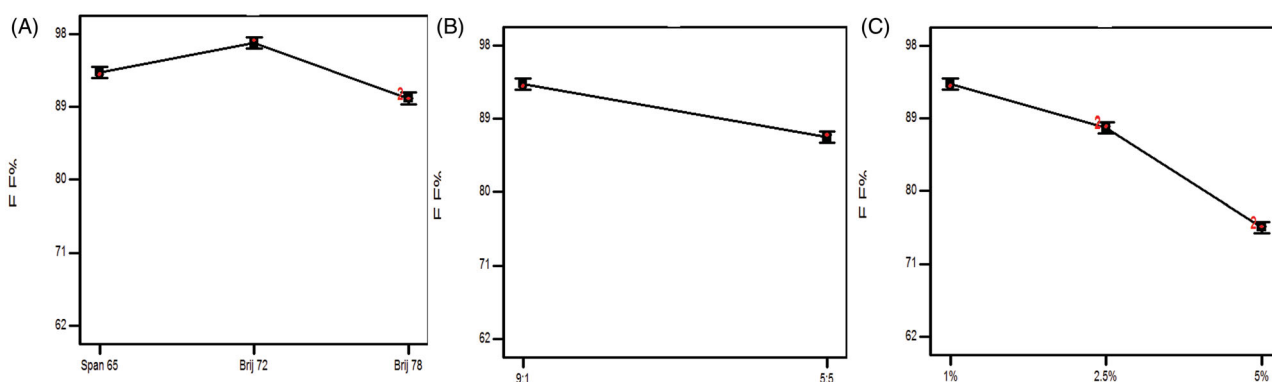


**Figure 2.** Effect of experimental variables on EE%: (A) effect of surfactant type, (B) effect of surfactant:cholesterol ratio, and (C) effect of bile salt concentration.

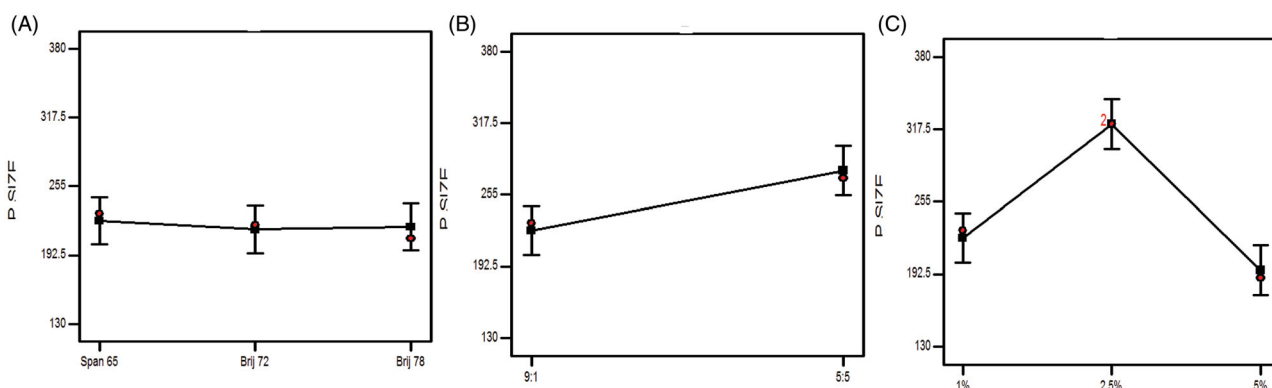


**Figure 3.** Effect of experimental variables on particle size. (A) Effect of surfactant type, (B) effect of surfactant:cholesterol ratio, and (C) effect of bile salt concentration.

increase in the amount of cholesterol and the improved drug inclusion within the bilosomes might be associated with an elevation in the size of the vesicles.

### 3.3.3. Influence of bile salt concentration

There was a significant ( $p < .0001$ ) elevation in the particle size associated with the increase in the bile salt concentration. The high negativity imparted on the vesicles owing to the anionic nature of SDC, the repulsion between the bilosomal vesicles will be increased, hence, vesicles of larger sizes will be obtained (El Zaafarany et al., 2010). Furthermore, there is a structure similarity between the bile salt and steroids, which in consequence enlarge the size due to its bulkiness (Salama et al., 2012). Interestingly, the further increase in the concentration to 5% predispose to diminish in the size, owing to the negative effect on the membrane rigidity, increasing the drug leakage, thus, decrease the size, also at higher concentrations micelles might be formed which are of smaller sizes (Albash et al., 2019).

### 3.4. PDI and ZP

The homogeneity and monodispersity can be figured out by the value of PDI, where a PDI of value zero denotes monodispersity, meanwhile PDI of value 1 denotes polydispersity. The PDI of the prepared piperine-loaded bilosomal formulae as illustrated in Table 3 ranged from  $0.22 \pm 0.02$  to  $0.64 \pm 0.12$ .

So they allied toward polydispersity but within appropriate range (Stetefeld et al., 2016).

ZP is a method of assessment the degree of stability of the colloidal systems as it estimates the net charges adopted. Generally, ZP values around  $\pm 30$  mV denote the stability of the system due to the ensured electric repulsion between the vesicles (Al-mahallawi et al., 2015). In the current experiment, the measured ZP values from bilosomes ranged from  $-32.3 \pm 3.4$  to  $-53.3 \pm 5.4$  mV (Table 3). The high negativity was acquired due to the anionic nature of the bile salt included in the construction of the bilosomes (Dai et al., 2013).

### 3.5. Influence of the variables on Q8hr

The percent of piperine released after 8 h ranged from  $75.2 \pm 2.5$  to  $102.3 \pm 2.5$  (Table 3). The impact of the variables, surfactant type (A), surfactant:cholesterol ratio (B), and bile salt concentration (C) on Q8hr is displayed as 3D response plot in Figure 1(C). The ANOVA statistical analysis revealed that the impact of interaction among AB, AC, and BC was non-significant ( $p > .05$ ). The linear impact of the variables was latterly discussed based on ANOVA results was graphically exploited in Figure 4. Furthermore, Figure 5(A–D) illustrates the release profiles of piperine from the fabricated bilosomes at different time intervals.

The release profile of the fabricated bilosomes exhibited a dual consecutive phases: phase I allocated in the first couple



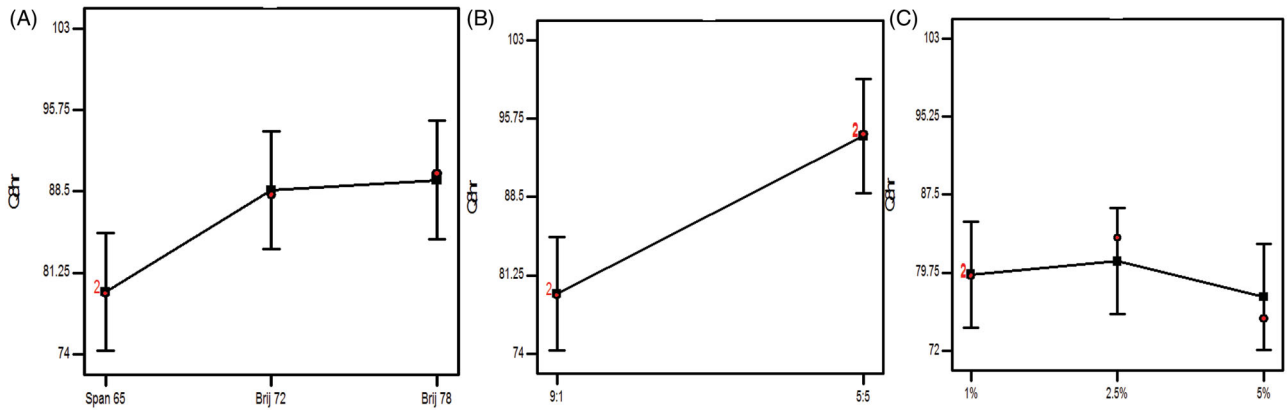


Figure 4. Effect of experimental variables on Q8hr. (A) Effect of surfactant type, (B) effect of surfactant:cholesterol ratio, and (C) effect of bile salt concentration.

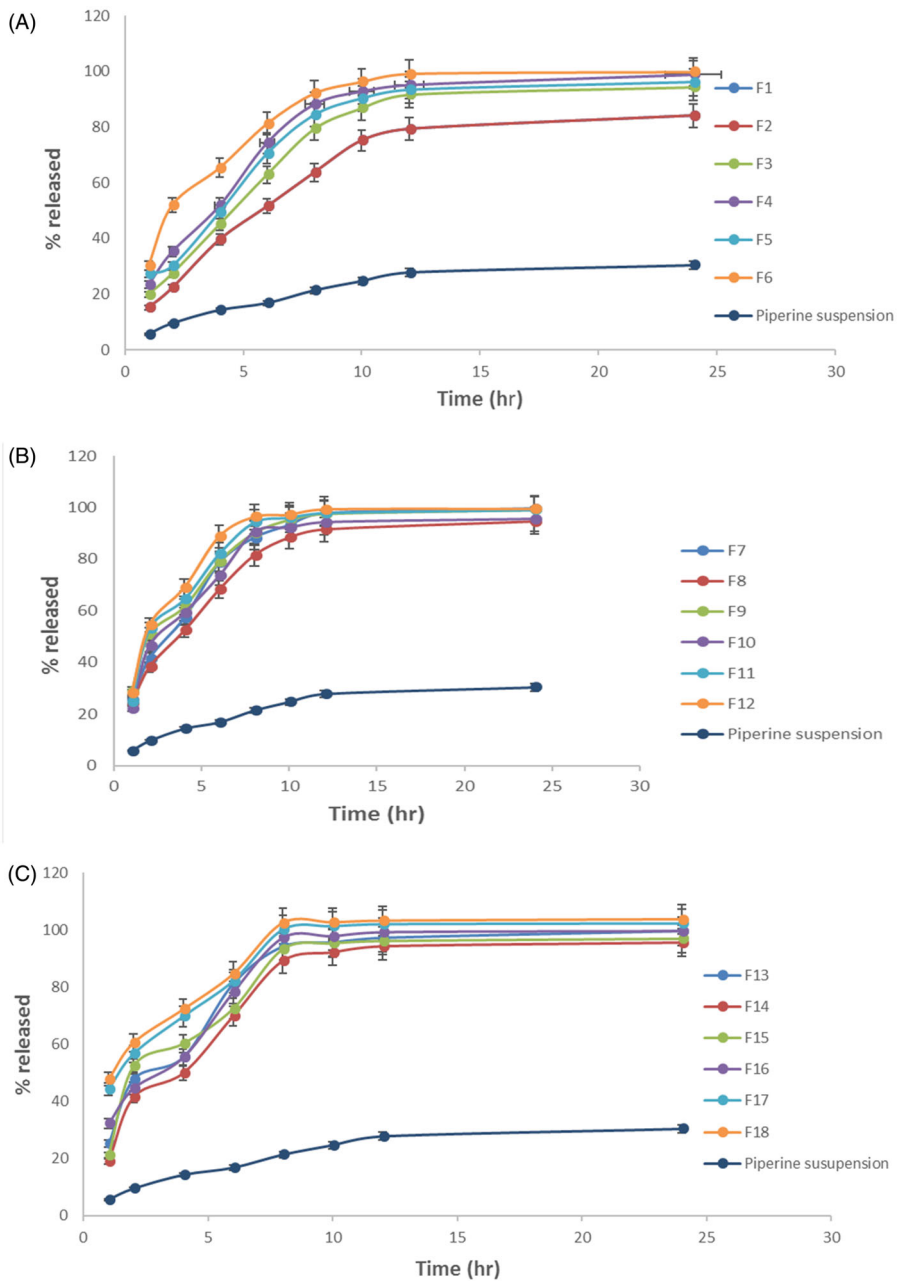


Figure 5. (A–C) Percent of piperine released  $\pm$  SD from the prepared formulae (F1–F18) compared to that of piperine suspension.

of hour, with rapid release of the drug ranged from 18% to 60% followed by phase II a slow drug release, moreover, the percent of drug release is highly correlated with the percent of free drug which can be easily evolved than that included in the hydrophobic pockets in the vesicles.

### 3.5.1. Influence of surfactant type

Since the drug release is highly dependent on the amount of drug entrapped, this in accordance of the results of ANOVA statistical analysis, the formulae prepared using span 65 and Brij 72 exploited the significantly ( $p < .05$ ) smaller Q8hr than those prepared by Brij 78 using. Furthermore surfactants of low HLB and higher  $T_c$  will predispose to the formation of more tightly packed vesicles and increasing the membrane fluidity (Aboelwafa et al., 2010).

### 3.5.2. Influence of surfactant:cholesterol ratio

Also increasing the amount of cholesterol predisposes to increase membrane compactness and decrease the drug permeation. Unfortunately, this will happen to a certain limit after that the cholesterol will displace the drug in the hydrophobic voids increasing its leakage, hence, increasing the drug release. This agreed with our results where the Q8hr will be significantly ( $p = .0018$ ) increased when the ratio was 5:5 (Aboelwafa et al., 2010).

### 3.5.3. Influence of bile salt concentration

The results of changing the concentration of bile salt were not significant ( $p > .5$ ) as the bile salt SDC is highly hydrophobic, highly resembling the nature of the drug so that the drug will favor being conjugated to SDC in the formulae rather than being solubilized and released in the dissolution media. Furthermore, at higher concentrations, SDC micelles are characterized by noticeably smaller aggregation numbers and solubilization capacity due to the rigid structure of SDC molecules, their facial amphiphilicity, and a low value of hydrophilic-lipophilic balance (Bogdanova et al., 2012; Aburahma, 2014; Albash et al., 2019).

Based on the aforementioned data, F2 was composed of Brij 72. Surfactant:cholesterol ratio 9:1 and 1% SDC were revealed to be the optimum piperine-loaded bilosomal formula with a desirability value of approximately 0.801.

## 3.6. In vitro characterization of piperine-loaded bilosome optimum formula

### 3.6.1. DSC

DSC thermograms of pure piperine, cholesterol, plain lyophilized formula as well as the optimum lyophilized piperine-loaded bilosomal formula (F2) were displayed in Figure 6. DSC thermogram of pure piperine revealed an acute pointed distinctive endotherm at approximately 131.2 °C which is equivalent to its melting point (Ding et al., 2018), while cholesterol exhibited an endothermic peak at 148.5 °C corresponding to its melting point (Abdelbary et al., 2018). DSC thermogram of lyophilized plain and piperine-loaded bilosomal formula (F2) exhibited no characteristic peak of piperine suggesting the complete transaction of piperine and other components as Brij 72, SDC, and cholesterol from a crystalline to amorphous form proposing good encapsulation of the drug within the vesicles.

### 3.6.2. Transmission electron microscope TEM

The array of TEM as obviously appeared in Figure 7 assured that the bilosomal vesicles were spherical and no vesicles with irregular shape were visible. In addition, TEM image demonstrated that the vesicles had a smooth surface excluding any drug crystal conforming the complete transformation of the drug into amorphous configuration and it came in accordance with the results of DSC.

### 3.6.3. Stability study

The results of stability study of the optimum piperine-loaded bilosome (F2) post 3 and 6 months of storage at 4 °C and 25 °C revealed that no significant changes happened to the estimated parameters: EE%, particle size, and Q8hr (Table 5). This may be attributed to the dense negativity of the fabricated vesicles, owing to the inclusion of the bile salt (SDC), thus, prohibiting the lumping of the vesicles. Furthermore, the high transition phase temperature and low HLB of the surfactant predispose to the configuration of closely packed vesicles, thus, prohibiting the drug leakage (Vora et al., 1998).

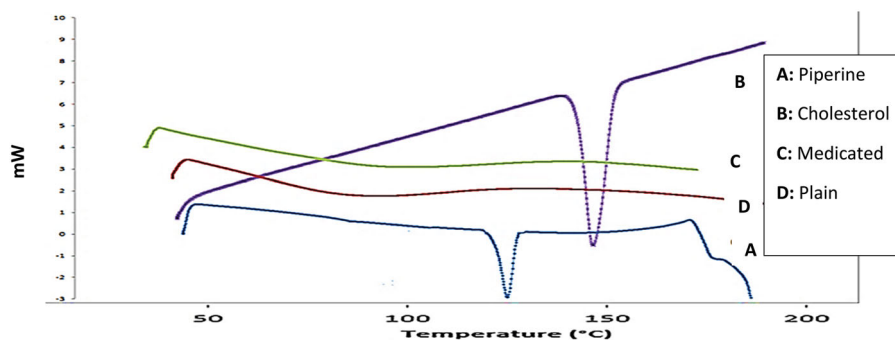


**Figure 6.** DSC thermograms. (A) Thermogram of pure piperine, (B) thermogram of cholesterol, (C) thermogram of plain formula (F2), and (D) thermogram of the optimum piperine-loaded bilosome (F2).

### 3.7. Ex vivo piperine gut permeation study

In the proceeded study, non-everted gut sac technique was adopted to assess the intestinal lavage of piperine via comparing the optimum piperine-loaded formula (F2) with piperine suspension in a trial to simulate the *in vivo* model to prospect the biological and kinetic availability of the drug. Post 90 minutes' experiment, it was revealed that optimized bilosomal formula (F2) revealed greater flux  $J_{max}$  of the optimized bilosomal formula =  $1.31 \pm 0.057 \mu\text{g}/\text{cm}^2/\text{min}$  compared to  $J_{max}$  of piperine suspension =  $0.297 \pm 0.0156 \mu\text{g}/\text{cm}^2/\text{min}$  and the apparent permeability of piperine formula (F2) was  $p_{app} = 5.3 \times 10^{-4} \text{cm}/\text{min}$ , meanwhile that of

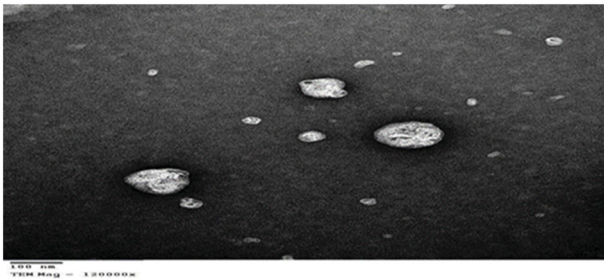


Figure 7. Transmission electron microscope image of optimum piperine-loaded bilosome.

piperine suspension  $1.2 \times 10^{-4} \text{cm}/\text{min}$ , denoting a significant superior ( $p < .05$ ) permeation of F2 over piperine suspension about 4.4 times increment (Figure 8(A)). The results exploited in Figure 8(B) refer to the superiority of F2 over the drug suspension at all-time intervals and this is a consequence of the minute size of the vesicle and full inclusion of piperine in the vesicles, thus, it can bypass freely any obstacle hindering its absorption (Sallam & Marin, 2015)

### 3.8. In vitro anti-MERS-CoV activity assessment

#### 3.8.1. MTT cytotoxicity assay ( $TC_{50}$ )

The assessment of the cytotoxicity of an antiviral drug is a crucial issue to assure the safety for the host to prohibit either acute or long-term toxicity (Badria et al., 2020). A beneficial antiviral should compromise between activity at diminished concentration and being cytotoxic at elevated concentration. Figure 9 reveals that  $TC_{50}$  of both F2 was  $2.29 \mu\text{g}/\text{ml}$ , while that of piperine suspension was  $0.6 \mu\text{g}/\text{ml}$ . Also it can be depicted that F2 adopts significant higher ( $p < .05$ )  $TC_{50}$  than piperine suspension, thus, the safety margin of F2 was superior by around 3.8 times over piperine suspension. Furthermore, those  $TC_{50}$  were utilized in customizing the safe serial dilutions used later in plaque assay.

Table 5. The effect of storage on the physical characteristics of F2 [all values exploited as mean  $\pm$  SD ( $n=3$ ), @ non-significant difference at ( $p > 0.05$ ) compared to that of fresh F2].

Parameter	Fresh F2	F2 post 3M at 4 °C	F2 post 3M at 25 °C	F2 post 6M at 4 °C	F2 post 6M at 25 °C
EE%	97.5 $\pm$ 0.8	97.1 $\pm$ 1.2 <sup>@</sup>	96.1 $\pm$ 1.8 <sup>@</sup>	94.5 $\pm$ 2.2 <sup>@</sup>	93.8 $\pm$ 1.6 <sup>@</sup>
Particle size	221.4 $\pm$ 16.5	222.1 $\pm$ 10.2 <sup>@</sup>	224.5 $\pm$ 5.4 <sup>@</sup>	227.7 $\pm$ 7.9 <sup>@</sup>	228.9 $\pm$ 5.9 <sup>@</sup>
Q8hr	88.8 $\pm$ 6.7	88.9 $\pm$ 8.5 <sup>@</sup>	90.5 $\pm$ 5.7 <sup>@</sup>	92.2 $\pm$ 4.6 <sup>@</sup>	94.3 $\pm$ 7.2 <sup>@</sup>

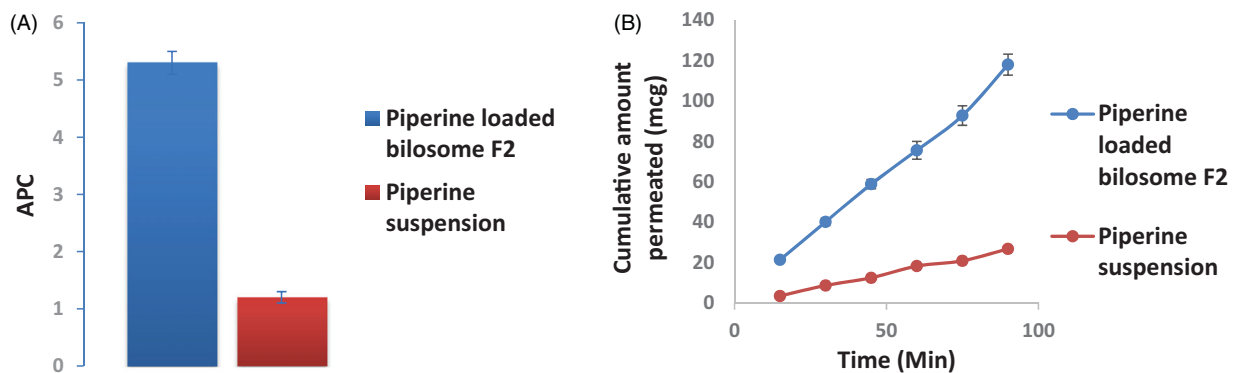


Figure 8. Piperine *ex vivo* gut permeation study exploiting; (A)  $P_{app} \pm$  S.D. of piperine-loaded bilosome (F2) versus piperine suspension and (B) cumulative amount of piperine permeated (mcg)  $\pm$  SD of piperine-loaded bilosome (F2) versus piperine suspension time profile.

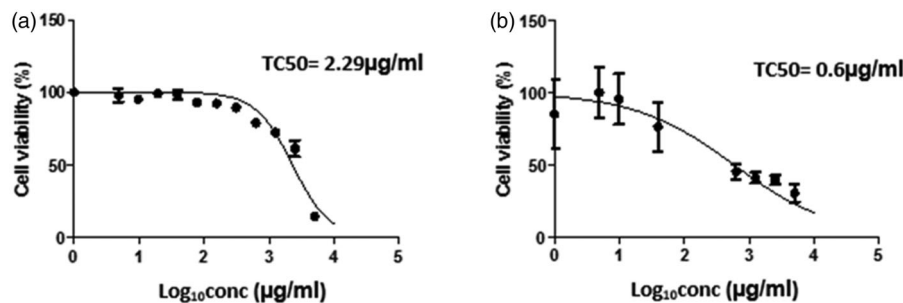


Figure 9. *In vitro* cytotoxicity of (A) piperine-loaded bilosome F2 and (B) piperine suspension.

### 3.8.2. Plaque assay

The viral plaque assay results are graphically exploited in Figure 10 and it can be depicted that F2 was capable of prohibiting viral plaque by  $83.4\% \pm 4.2$  at a concentration of  $0.25 \mu\text{g/ml}$ , while piperine suspension inhibits the viral plaque by  $33.2\% \pm 1.6$  at a concentration of  $0.25 \mu\text{g/ml}$ . From the results, it can be denoted that piperine has an antiviral activity at low concentration; furthermore, the antiviral activity against MERS-CoV-loaded vero E6 cell of F2 ( $EC_{50} = 0.141 \mu\text{g/ml}$ ) was significantly superior ( $p < .005$ ) over piperine suspension ( $EC_{50} = 0.376 \mu\text{g/ml}$ ). The promoted antiviral activity might be accredited to the possible interaction of the formulated vesicles with viral cells by fusion or endocytosis. The

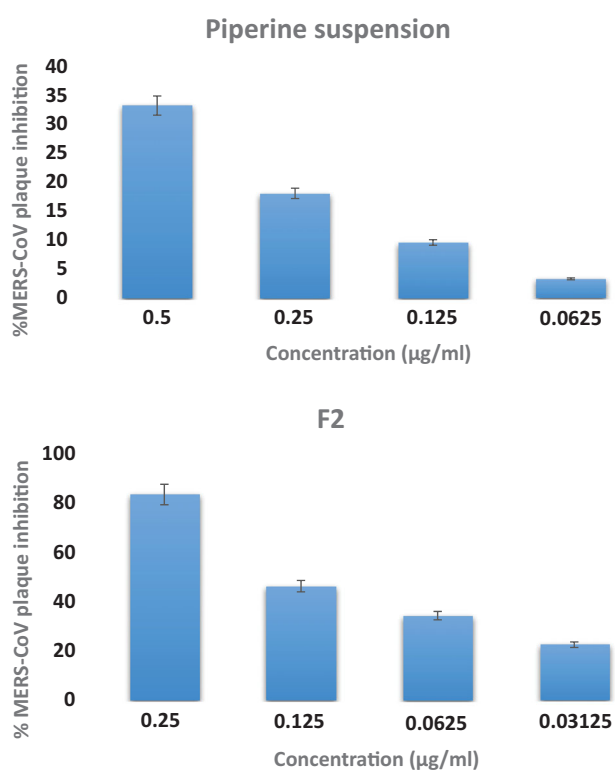


Figure 10. Piperine MERS-CoV plaque assay  $\pm$  SD: F2 and piperine suspension.

focused promoted thermodynamic activity gradient of piperine at the cellular interface as a result of bilosomal vesicles adhesion onto the membrane surface predispose to a higher permeation of lipophilic species. Also the surfactants incorporated in the fabrication of the bilosomes have a crucial effect in enhancing piperine permeation across the viral cells (Badria et al., 2020). These results came in accordance with various studies that report the impact vesicular system as proniosomes in enhancing antiviral activity of curcumin against HSV (El-Halim et al., 2020). Additionally, selectivity index (SI) is computed by dividing the concentration of 50% cellular cytotoxicity to 50% effective concentration ( $SI = CC_{50}/EC_{50}$ ), denoting the comparative efficacy of a compound in viral replication inhibition to its cytopathic effect (Cong et al., 2018). Curiously, the SI value of F2 (15.8) was significantly superior ( $p < .05$ ) than piperine suspension (1.59), denoting the promoted selectivity of F2.

### 3.9. Molecular docking study

Piperine was investigated for molecular docking into the active site of the Middle East respiratory syndrome coronavirus (PDB code: 4L3N) using Molecular Operating Environment (MOE) to show the binding mode of this molecule. Figure 11 reveals the results of binding interaction, demonstrating strong binding of piperine with the active site of the target 4L3N receptor. Piperine interacted by its oxygen atom of benzodioxole ring as the H-bond donor with the key amino acid Thr 477. In addition, the hydrophobicity induced by piperine resulted in a docking score of  $-16.7 \text{ kcal/mol}$ . Accordingly, from the obtained results, it is clear that piperine exhibits a high antiviral activity against MERS-CoV confirmed by its high binding affinity to RBD responsible for binding to the host receptor and subsequently fusing viral and host membranes, hence, coronavirus enters into host cells (Tai et al., 2017).

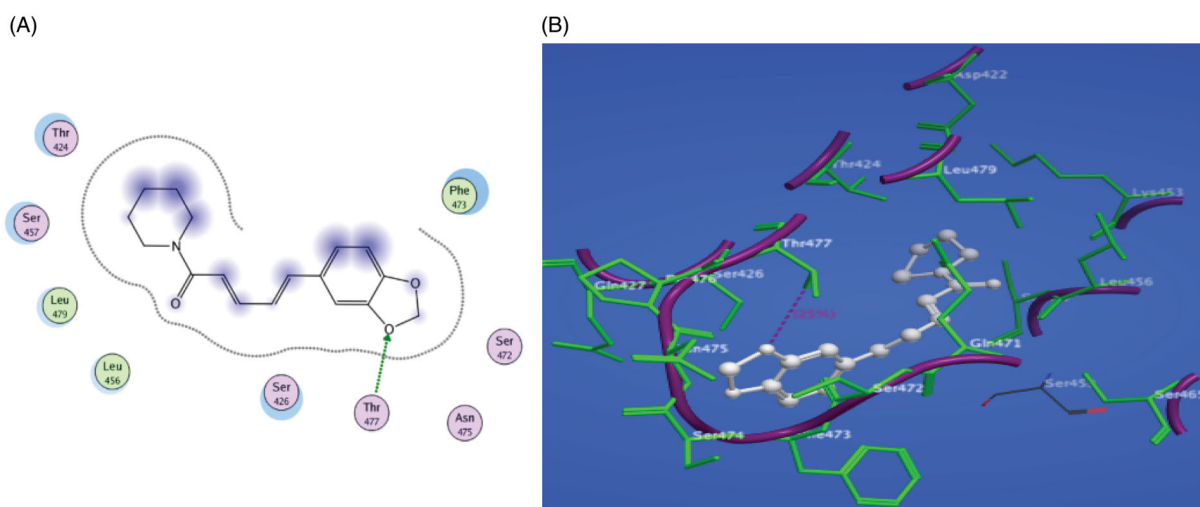


Figure 11. (A) 2D representation of piperine docking inside the active site of 4L3N. (B) 3D representation of piperine docking inside the active site of 4L3N.



### 3.10. In vivo study

The influence of piperine on MERS-CoV-induced mice infection was assessed and the difference in the effect of the optimum piperine-loaded bilosome F2 versus piperine suspension was investigated.

Basically, MERS-CoV infection predispose to drastic pathological changes including lymphoid infiltration and interstitial inflammation also noticed (Saadat et al., 2019). Moreover, it encourages the oxidative damage associated with the elevation in MDA levels and the depletion in total thiol concentration as well as GSH, SOD, and CAT activities in the serum. It can be depicted that IL-4 level will be diminished and the levels of IFN- $\gamma$ , TGF- $\beta$ 1, and PGE2 in the lung lavage will be boosted owing to this infection. Moreover, the tremendous evolution of IFN- $\gamma$  and ILs over the course of the infection was dramatic, denoting the induction of a massive antiviral response upon MERS-CoV infection.

Hence, in this proceeded study, not only the antiviral effect of piperine but also the anti-inflammatory and antioxidant effect was confirmed via the estimation of BALF levels of IL-4 and INF- $\gamma$  and serum levels of GSH and MDA to exploit the capability of piperine to diminish the harsh consequences of MERS-CoV infection.

#### 3.10.1. Estimation of the viral titer in acutely infected lungs via plaque assay

It was reported that the virus can be distinguished in the respiratory tract of C57BL/6 mice at 6 h post-infection, while it sparsely to be detected 7 day post-infection (Iwata-Yoshikawa et al., 2019). Hence, the duration of the

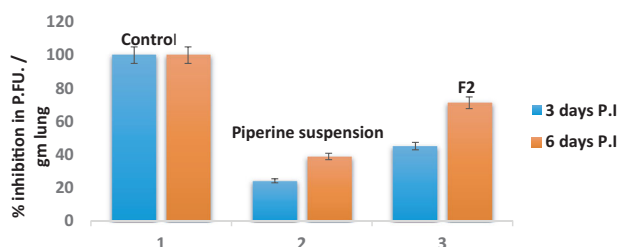


Figure 12. MERS-CoV titer in lung homogenate via plaque assay  $\pm$  SD at days 3 and 6 post-infection after treatment of either F2 and piperine suspension.

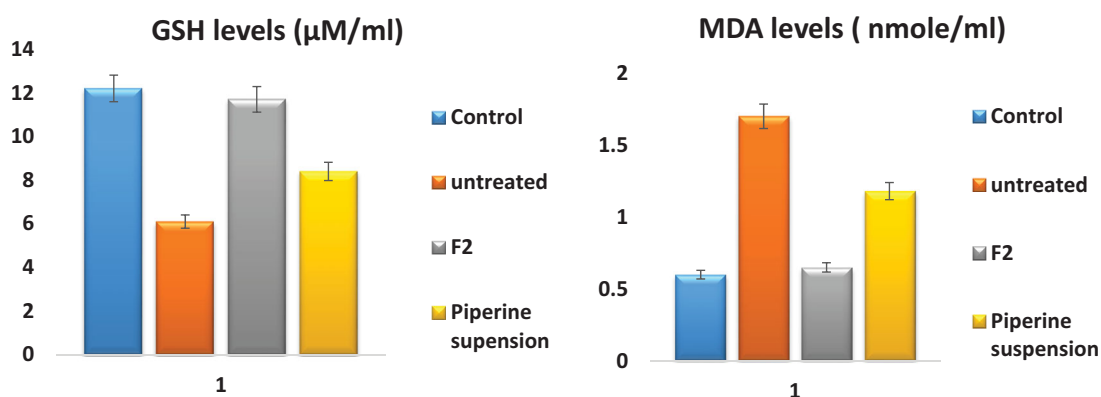


Figure 13. GSH and MDA levels  $\pm$  SD in serum; control group, infected without treatment, infected with F2 treatment, and infected with piperine suspension treatment.

experiment not exceeding 6 days post-infection. From the findings in Figure 12, it can be depicted that the percent of plaque inhibition of F2 at days 3 and 6 post-infection (45.1% and 71.2%), respectively, was significantly superior compared to that of piperine suspension (24% and 38.7%), respectively.

#### 3.10.2. Assessment of serum oxidant and antioxidant biomarkers

The serum level of MDA was elevated to  $1.7 \pm 0.16 \mu$ M post-MERS infection compared to its level in the control group  $0.6 \pm 0.07 \mu$ M, denoting the evolution of oxidative stress, hence, elevation of MDA levels. Meanwhile, its level after administration of piperine was declined to  $0.65 \pm 0.14 \mu$ M in the case of F2 and  $1.18 \pm 0.2$ . From the results, it was revealed that F2 significantly ( $p < .001$ ) decrease the levels of MDA than that of the untreated and piperine suspension receiving group.

Furthermore, the serum level of GSH was depleted to  $6.1 \pm 0.7 \mu$ M post-infection administration compared to its level in the control group  $12.4 \pm 1.5 \mu$ M, this decline was significantly ( $p < .001$ ) reversed after administration of piperine reaching to  $11.7 \pm 1.2 \mu$ M in the case of F2 while in the case of piperine suspension  $8.4 \pm 0.9 \mu$ M, these results configured in Figure 13 were confirmed by previously conducted studies (Mittal & Gupta, 2000).

#### 3.10.3. Assessment of IL-4 and IFN- $\gamma$ in BALF

The BALF level of IFN- $\gamma$  was elevated to  $120.1 \pm 13.2$  pg/mg protein post-infection administration compared to its level in the control group  $41.25 \pm 6.07$  pg/mg protein, denoting the emerging of the inflammatory storm, hence, up regulation of IFN- $\gamma$  levels. Meanwhile, its level after administration of piperine was down expressed to  $45.4 \pm 7.51$  pg/mg protein in the case of F2 and  $81.4 \pm 6.2$  pg/mg protein in the case of piperine suspension. From the results, it was revealed that F2 significantly ( $p < .001$ ) decreases the levels of IFN- $\gamma$  than that of the untreated and piperine suspension receiving group.

Eventually, the down regulation of IL-4 level in BALF as a consequence of the inflammatory response is associated with the MERS-CoV infection  $15.7 \pm 2.7$  pg/mg protein instead of  $36.3 \pm 3.52$  pg/mg protein in the control group.

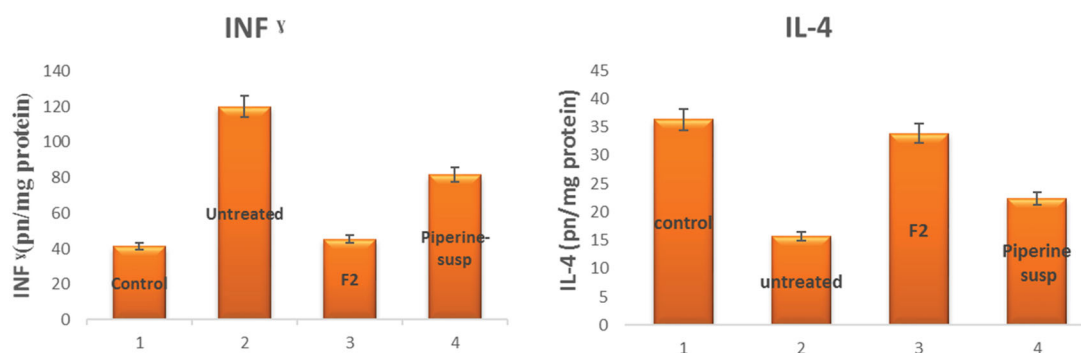


**Figure 14.** INF- $\gamma$  and IL-4 levels  $\pm$ SD in BALF; (1) control group, (2) untreated, (3) infection with F2 treatment, and (4) infection with piperine suspension treatment.

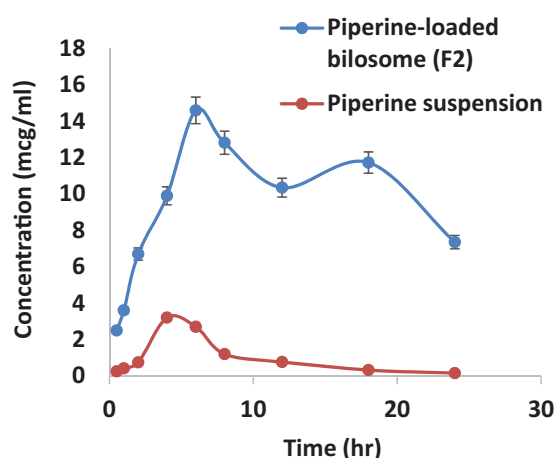


**Figure 15.** Pharmacokinetic profiles of piperine versus time  $\pm$ SD after oral administration of F2 and piperine suspension.

**Table 6.** Pharmacokinetic parameters of piperine post the oral administration of F2 and piperine suspension.

Pharmacokinetic parameter	F2	Piperine suspension
$C_{max}$ (mcg/ml)	$14.62 \pm 1.7^{**}$	$3.21 \pm 0.65$
$T_{max}$ 1 (h)	6 <sup>**</sup>	4
$T_{max}$ 2 (h)	18	–
$AUC_{[0-24]}$ (mcg h/ml)	$440.39 \pm 60.4^{**}$	$70.35 \pm 12.2$
$AUC_{[0-\infty]}$ (mcg h/ml)	$461.8 \pm 65.2$	$76.5 \pm 12.5$

Data exploited as mean  $\pm$  SD,  $n = 6$ , <sup>\*\*</sup>significant difference at  $p < .05$ .

Meanwhile, after administration of piperine, IL-4 levels were upregulated significantly at  $p < .001$  to  $33.84 \pm 2.82$  pg/mg in the case of F2 and  $22.3 \pm 1.2$  pg/mg. The results are represented in Figure 14 and affirmed by the results stated in previously conducted studies (Wang-Sheng et al., 2017).

### 3.11. Pharmacokinetic study

Figure 15 reveals the plasma concentration–time profiles of the optimized piperine-loaded bilosomes (F2) and piperine suspension. As depicted from Table 6, the pharmacokinetic parameters of F2 were significantly ( $p < .05$ ) superior over piperine suspension. As piperine-loaded bilosomes (F2) exhibited  $C_{max}$  of  $14.62 \pm 1.7$  mcg/ml which was significantly higher ( $p < .05$ ) than that of piperine suspension ( $3.21 \pm 0.65$  mcg/ml). In addition, F2  $T_{max}$  value was significantly prominent compared to that of piperine suspension, this may be attributed to the prolonged piperine release

from the vesicles. Furthermore,  $AUC_{[0-24]}$  of F2 bilosomes was estimated to be  $440.39 \pm 60.4$  mcg h/ml which was highly significant ( $p < .05$ ) compared to  $AUC_{[0-24]}$  of piperine suspension ( $70.35 \pm 12.2$  mcg h/ml).

The enhanced permeation of piperine across GIT segments predisposes to 6.2-folds' significant increase in the relative bioavailability of F2 compared to the drug suspension. From Figure 15, it was noticed the characterization of double peak and this happened to the drugs eliminated via hepato-enteric circulation. Piperine eliminated by bile excretion and enterohepatic circulation leading to a portion of the drug will be reabsorbed and this is in accordance with previously conducted studies (Shao et al., 2015).

These findings capitulate the harsh antiviral activity of the piperine. Moreover, piperine is a crucially oppose the emerged free radicals and cytokines associated with the inflammatory and oxidative damage. These results figure out to the enhanced antiviral activity of piperine-loaded bilosome over piperine suspension. Owing to these characteristics, piperine-loaded bilosome can be successfully attempted as a therapeutic compound or prophylactic to prohibit the harsh inflammation and the oxidative stress induced during the MERS-CoV and COVID-19 infection.

## 5. Conclusions

In the current study, bilosomes were scrutinized as a nanovesicular carriers for oral delivery of piperine as an impressive antiviral and anti-inflammatory. Eighteen formulae were fabricated in accordance to  $3^2 \cdot 2^1$  full factorial design. F2 was picked as the optimum formula on the fundamental of EE%, particle size, and Q8hr. F2 exhibited the highest EE%, smaller particle size, and restrained drug release. *Ex vivo* and pharmacokinetic studies revealed the significant superior drug permeation from F2 over piperine suspension. F2 exhibited a higher safety margin and efficacy as antiviral correlated to piperine suspension. Likewise, F2 manifested a massive role versus MERS-CoV induced inflammation, besides its prevailing antioxidant effect, F2 was superior not only over piperine suspension as an antiviral but also in the anti-inflammatory and antioxidant activity. As a consequence, the findings affirmed that optimum piperine-loaded bilosome F2 could as a crucial panel in oral delivery of piperine and to be adopted

as a prophylactic or therapeutic agent to abolish the exaggerated consequences of MERS-Cov and COVID 19 infection.

## Acknowledgments

The authors thank Prof. Dr Mohamed A. A. Ali, PhD, Director of Center of Scientific Excellence for Influenza Viruses National Research Centre 12311 Dokki, Giza, Egypt, for his persistent and generous help in the virology part of this study. Also the authors thank the Deanship of Scientific Research at Taif University for funding this work through Taif University Researchers Supporting Project number (TURSP-2020/222), Taif University, Taif, Saudi Arabia.

## Disclosure statement

The authors declare no conflict of interest regarding the publication of this paper.

## Funding

Taif University Researchers Supporting Project number (TURSP-2020/222), Taif University, Taif, Saudi Arabia.

## References

- Abdelbary GA, Amin MM, Zakaria MY, El Awdan SA. (2018). Adefovir dipivoxil loaded proliposomal powders with improved hepatoprotective activity: formulation, optimization, pharmacokinetic, and biodistribution studies. *J Liposome Res* 28:259–74.
- Abdellatif MM, Khalil IA, Khalil MAF. (2017). Sertaconazole nitrate loaded nanovesicular systems for targeting skin fungal infection: in-vitro, ex-vivo and in-vivo evaluation. *Int J Pharm* 527:1–11.
- Aboelwafa AA, El-Setouhy DA, Elmeshad AN. (2010). Comparative study on the effects of some polyoxyethylene alkyl ether and sorbitan fatty acid ester surfactants on the performance of transdermal carvedilol proniosomal gel using experimental design. *AAPS PharmSciTech* 11: 1591–602.
- Abou-Karam M, Shier WT. (1990). A simplified plaque reduction assay for antiviral agents from plants. Demonstration of frequent occurrence of antiviral activity in higher plants. *J Nat Prod* 53:340–4.
- AbouSamra MM, Salama AH. (2017). Enhancement of the topical tolnaftate delivery for the treatment of tinea pedis via provesicular gel systems. *J Liposome Res* 27:324–34.
- Aburahma MH. (2014). Bile salts-containing vesicles: promising pharmaceutical carriers for oral delivery of poorly water-soluble drugs and peptide/protein-based therapeutics or vaccines. *Drug Deliv* 1–21: 1847–67.
- Albash R, El-Nabarawi MA, Refai H, Abdelbary AA. (2019). Tailoring of PEGylated bilosomes for promoting the transdermal delivery of olmesartan medoxomil: in vitro characterization, ex-vivo permeation and in-vivo assessment. *Int J Nanomed*. 14: 6555–74.
- Al-mahallawi AM, Abdelbary AA, Aburahma MH. (2015). Investigating the potential of employing bilosomes as a novel vesicular carrier for transdermal delivery of tenoxicam. *Int J Pharm* 485:329–40.
- Alshehri S, Imam SS, Hussain A, Altamimi MA. (2020). Formulation of piperine ternary inclusion complex using  $\beta$  CD and HPMC: physicochemical characterization, molecular docking, and antimicrobial testing. *Processes* 8:1450.
- Ammar HO, Ibrahim M, Mahmoud AA, et al. (2018a). Non-ionic surfactant based in situ forming vesicles as controlled parenteral delivery systems. *AAPS PharmSciTech* 19:1001–10.
- Ammar HO, Mohamed MI, Tadros MI, Fouly AA. (2018b). Transdermal delivery of ondansetron hydrochloride via bilosomal systems: in vitro, ex vivo, and in vivo characterization studies. *AAPS PharmSciTech* 19: 2276–87.
- Badria FA, Abdelaziz AE, Hassan AH, et al. (2020). Development of provesicular nanodelivery system of curcumin as a safe and effective antiviral agent: statistical optimization, in vitro characterization, and antiviral effectiveness. *Molecules* 25:5668.
- Bajad S, Singla AK, Bedi KL. (2002). Liquid chromatographic method for determination of piperine in rat plasma: application to pharmacokinetics. *J Chromatogr B* 776:245–9.
- Bnyan R, Khan I, Ehtezazi T, et al. (2018). Surfactant effects on lipid-based vesicles properties. *J Pharm Sci* 107:1237–46.
- Bogdanova LR, Gnezdilov OI, Ildiyatullin BZ, et al. (2012). Micellization in sodium deoxycholate solutions. *Colloid J* 74:1–6.
- Chen Y, Rajashankar KR, Yang Y, et al. (2013). Crystal structure of the receptor-binding domain from newly emerged Middle East Respiratory Syndrome Coronavirus. *J Virol* 87:10777–83.
- Chopra B, Dhingra AK, Kapoor RP, Prasad DN. (2016). Piperine and its various physicochemical and biological aspects: a review. *CHEM* 3: 75–96.
- Coates BM, Staricha KL, Koch CM, et al. (2018). Inflammatory monocytes drive Influenza A virus-mediated lung injury in juvenile mice. *J Immunol* 200:2391–404.
- Cockrell AS, Yount BL, Scobey T, et al. (2017). A mouse model for MERS coronavirus-induced acute respiratory distress syndrome. *Nat Microbiol* 2:16226.
- Cong Y, Hart BJ, Gross R, et al. (2018). MERS-CoV pathogenesis and antiviral efficacy of licensed drugs in human monocyte-derived antigen-presenting cells. *PLoS One* 13:e0194868.
- Dai Y, Zhou R, Liu L, et al. (2013). Liposomes containing bile salts as novel ocular delivery systems for tacrolimus (FK506): in vitro characterization and improved corneal permeation. *Int J Nanomedicine* 8: 1921–33.
- Damanhoury ZA. (2014). A review on therapeutic potential of Piper nigrum L. (Black Pepper): the king of spices. *Med Aromat Plants* 3:161.
- Ding Y, Wang C, Wang Y, et al. (2018). Development and evaluation of a novel drug delivery: Soluplus<sup>®</sup>/TPGS mixed micelles loaded with piperine *in vitro* and *in vivo*. *Drug Dev Ind Pharm* 44:1409–16.
- El Zaafarany GM, Awad GA, Holayel SM, Mortada ND. (2010). Role of edge activators and surface charge in developing ultra-deformable vesicles with enhanced skin delivery. *Int J Pharm* 397:164–72.
- El-Halim SMA, Mamdouh MA, El-Haddad AE, Soliman SM. (2020). Fabrication of anti-HSV-1 curcumin stabilized nanostructured proniosomal gel: molecular docking studies on thymidine kinase proteins. *Sci Pharm* 88:9.
- Elnaggar YSR, Omran S, Hazzah HA, Abdallah OY. (2019). Anionic versus cationic bilosomes as oral nanocarriers for enhanced delivery of the hydrophilic drug risenedronate. *Int J Pharm* 564:410–25.
- Hathout RM, Mansour S, Mortada ND, Guinedi AS. (2007). Liposomes as an ocular delivery system for acetazolamide: in vitro and in vivo studies. *AAPS PharmSciTech* 8:1–E12.
- Henen MA, El Bialy SA, Goda FE, et al. (2012). [1,2,4]Triazolo[4,3-a]quinoxaline: synthesis, antiviral, and antimicrobial activities. *Med Chem Res* 21:2368–78.
- Imam SS, Alshehri S, Alzahrani TA, et al. (2020). Formulation and evaluation of supramolecular food-grade Piperine HP  $\beta$  CD and TPGS complex: dissolution, physicochemical characterization, molecular docking, in vitro antioxidant activity, and antimicrobial assessment. *Molecules* 25:4716.
- Iwata-Yoshikawa N, Okamura T, Shimizu Y, et al. (2019). Acute respiratory infection in human dipeptidyl peptidase 4-transgenic mice infected with Middle East Respiratory Syndrome Coronavirus. *J Virol* 93: e01818–18.
- Li K, McCray PB. (2020). Development of a mouse-adapted MERS Coronavirus. In: Vijay R, ed. *MERS Coronavirus, methods in molecular biology*. New York, NY: Springer US, 161–71.
- Lu H. n.d. Drug treatment options for the 2019-new coronavirus (2019-nCoV). *Biosci. Trends* 3.

- Mishra A, Pathak Y, Tripathi V. (2020). Natural compounds as potential inhibitors of novel coronavirus (COVID-19) main protease: an in silico study (preprint) (in review).
- Mittal R, Gupta RL. (2000). In vitro antioxidant activity of piperine. *Methods Find Exp Clin Pharmacol* 22:271–4.
- Mohammed S, Abdelbary G, Amin M, et al. (2020). Stabilized oral nanostructured lipid carriers of Adefovir Dipivoxil as a potential liver targeting: estimation of liver function panel and uptake following intravenous injection of radioiodinated indicator. *DARU J Pharm Sci* 28: 517–32.
- Mosallam S, Sheta NM, Elshafeey AH, Abdelbary AA. (2021). Fabrication of highly deformable bilosomes for enhancing the topical delivery of terconazole: in vitro characterization, microbiological evaluation, and in vivo skin deposition study. *AAPS PharmSciTech* 22:74.
- Mrityunjaya M, Pavithra V, Neelam R, et al. (2020). Immune-boosting, antioxidant and anti-inflammatory food supplements targeting pathogenesis of COVID-19. *Front Immunol* 11:570122.
- Pachauri M, Gupta ED, Ghosh PC. (2015). Piperine loaded PEG-PLGA nanoparticles: preparation, characterization and targeted delivery for adjuvant breast cancer chemotherapy. *J Drug Deliv Sci Technol* 29: 269–82.
- Ramana LN, Sethuraman S, Ranga U, Krishnan UM. (2010). Development of a liposomal nanodelivery system for nevirapine. *J Biomed Sci* 17: 1–9.
- Saadat S, Beheshti F, Askari VR, et al. (2019). Aminoguanidine affects systemic and lung inflammation induced by lipopolysaccharide in rats. *Respir Res* 20:96.
- Saifi Z, Rizwanullah M, Mir SR, Amin S. (2020). Bilosomes nanocarriers for improved oral bioavailability of acyclovir: a complete characterization through in vitro, ex-vivo and in vivo assessment. *J Drug Deliv Sci Technol* 57:101634.
- Salama HA, Mahmoud AA, Kamel AO, et al. (2012). Brain delivery of olanzapine by intranasal administration of transfersomal vesicles. *J Liposome Res* 22:336–45.
- Sallam MA, Marin MT. (2015). Optimization, ex vivo permeation, and stability study of lipid nanocarrier loaded gelatin capsules for treatment of intermittent claudication. *Int J Nanomedicine* 10:4459.
- Selvendiran K, Prince Vijeya Singh J, Sakthisekaran D. (2006). In vivo effect of piperine on serum and tissue glycoprotein levels in benzo(a)-pyrene induced lung carcinogenesis in Swiss albino mice. *Pulm Pharmacol Ther* 19:107–11.
- Shakeri F, Soukhtanloo M, Boskabady MH. (2017). The effect of hydroethanolic extract of *Curcuma longa* rhizome and curcumin on total and differential WBC and serum oxidant, antioxidant biomarkers in rat model of asthma. *Iran J Basic Med Sci* 20:155–65.
- Shao B, Cui C, Ji H, et al. (2015). Enhanced oral bioavailability of piperine by self-emulsifying drug delivery systems: in vitro, in vivo and in situ intestinal permeability studies. *Drug Delivery* 22:740–7.
- Stetefeld J, McKenna SA, Patel TR. (2016). Dynamic light scattering: a practical guide and applications in biomedical sciences. *Biophys Rev* 8:409–27.
- Stojanović-Radić Z, Pejčić M, Dimitrijević M, et al. (2019). Piperine-A major principle of black pepper: a review of its bioactivity and studies. *Appl Sci* 9:4270.
- Tai W, Wang Y, Fett CA, et al. (2017). Recombinant receptor-binding domains of multiple Middle East Respiratory Syndrome Coronaviruses (MERS-CoVs) induce cross-neutralizing antibodies against divergent human and camel MERS-CoVs and antibody escape mutants. *J Virol* 91:e01651–16.
- Vora B, Khopade AJ, Jain NK. (1998). Proniosome based transdermal delivery of levonorgestrel for effective contraception. *J Control Release* 54:149–65.
- Wang-Sheng C, Jie A, Jian-Jun L, et al. (2017). Piperine attenuates lipopolysaccharide (LPS)-induced inflammatory responses in BV2 microglia. *Int Immunopharmacol* 42:44–8.
- Zhang L-K, Sun Y, Zeng H, et al. (2020). Calcium channel blocker amlodipine besylate therapy is associated with reduced case fatality rate of COVID-19 patients with hypertension. *Cell Discov* 6:96.